SCAL FOR GAS RESERVOIRS: A CONTRIBUTION FOR BETTER EXPERIMENTS

Arjen Cense[1], Jules Reed[2], Patrick Egermann[3]
[1]A/S Norske Shell, [2]LR Senergy, [3]Storengy (ENGIE)

This paper was prepared for presentation at the International Symposium of the Society of Core Analysts held in Snowmass, Colorado, USA, 21-26 August 2016

ABSTRACT

Special core analysis for gas fields requires a different approach than for oil fields. Gas fields are mostly produced via pressure depletion. Saturation changes are not large during this process, except if water is flooding (parts of) the reservoir. Gas reservoirs are mostly water wet, which is, from a SCAL point of view and from a reservoir simulation point of view, a significant simplification compared to oil fields, where wettability is often a big uncertainty and has significant impact on the shape of the (imbibition) capillary pressure and relative permeability curves. However, although the required SCAL input for reservoir simulation may seem to be relatively simple, the design and do-ability of the SCAL experiments in the lab is challenging, due to compressibility and solubility effects of gas. In this paper, we discuss what laboratory experiments are appropriate for gas fields and how they should be performed to obtain maximum value. We discuss what the uncertainties in these experiments are and how uncertainties can be reduced.

INTRODUCTION

With the current low oil prices and the focus to reduce cost, investments in gas projects are becoming more attractive. The price of gas has not dropped nearly as much as that of oil, which makes gas producing fields economically more stable. In addition, at the last climate change summit in Paris, it was decided by leaders of 195 nations that they will cut their carbon emissions. Since gas emits lower carbon emissions than coal and crude, gas producing fields are potential candidates to decrease the pace of global warming until we can rely on renewable energy sources.

When a natural gas field is discovered, the initial distribution of gas can often be inferred from the primary drainage capillary pressure curves, from which the saturation height function, i.e. gas saturation as a function of height-above-free-water-level (HAFWL), can be established. If the water level has moved pre-production, because of a (temporary) breach in the seal or because of a hydrodynamic (flowing) aquifer, we need to use the imbibition capillary pressure curves to describe those parts of the reservoir where water has displaced gas, and where gas has become residual or trapped (Figure 1).

Most natural gas fields are produced by depletion, meaning that wells produce gas by lowering the reservoir pore pressure, until production becomes uneconomic. Gas reservoirs are generally water wet, as the rock has not been in contact with wettability altering hydrocarbon components such as resins and asphaltenes. The processes at play

during reservoir production are simple: saturations hardly change and gas is flowing at initial (or connate) water saturation. The gas relative permeability is determined as the endpoint gas relative permeability ($k_{rg}(S_{wi}$ or $S_{wc})$ - green point in Figure 2). The water is still immobile, hence water relative permeability is zero.

In cases where a (strong) aquifer is present, the aquifer will invade during pressure depletion (depicted by orange arrows in Figure 1). The water from the aquifer then displaces the gas to its endpoint (yellow point in Figure 2), while the gas becomes trapped at residual gas saturation (S_{gr}). We generally see that pressures in gas reservoir models are mostly sensitive to $k_{rg}(S_{wi})$. Ultimate recovery appears less sensitive to $k_{rg}(S_{wi})$, but is more a function of S_{gr} and the endpoint water relative permeability, $k_{rw}(S_{gr})$. The shape of the relative permeability curves (e.g. gas and water Corey) are considered to be less important.

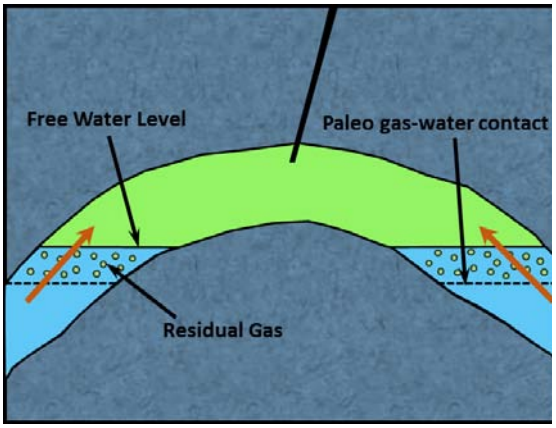

Figure 1: Schematic picture of gas reservoir with one producing well

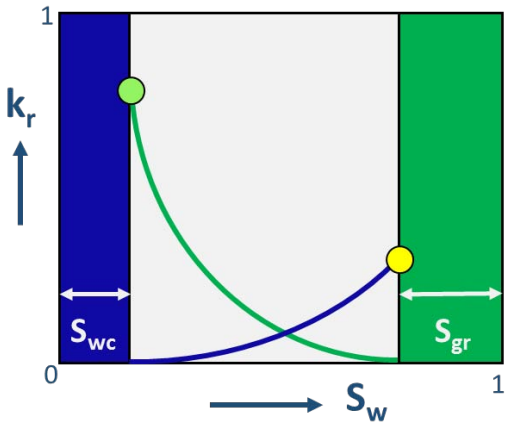

Figure 2: Relative permeability as function of water saturation

PITFALLS

Capillary Pressure

Generally speaking, the capillary pressure (Pc) curves are important to acquire because they have implications on both the volume of hydrocarbon in place and the sweep efficiency in the case of an active aquifer.

Gas In Place (GIP): the drainage Pc curves are usually the most relevant to evaluate the GIP, accounting for the transition zone especially for low-medium permeability range reservoirs. Nevertheless, for some reservoirs, the current Free Water Level (FWL) identified from the gas-brine pressure gradients can be different from the one prevailing several millions years before which is often referred to as paleo contact. In the situation where the paleo contact was shallower than the current contact, the system is still under gas filling process and therefore the drainage mode is still the relevant one (gas saturation increase). In the opposite situation, a paleo contact located deeper than the current contact means that the whole system has experienced a major imbibition process. It is therefore important to keep in mind that drainage Pc curves are not always the relevant curves for

GIP evaluation. There are two types of information that can provide indications about the possible paleo contact:

- non-zero gas saturation below the FWL, from pressure gradient measurements, indicating gas saturation values typically in the trapped gas saturation range (20-40%).
- gas saturation in the transition zone not properly reproducible by a drainage J-function.

An illustration of such paleo contact data is provided in Figure 3. In this case, a strong deviation from the drainage J-function trend was clearly observed in a depth window up to 12 ft above the FWL (left plot). Above this depth, the deviation between imbibition and drainage curves is narrower, in the asymptotic part (right plot) of the Pc curve. In this case, the transition zone impact was of limited extent because of favorable permeability, but it can lead to much more pronounced deviation for lower permeability reservoirs. For flat and extended reservoirs, the volume impact of using a drainage instead of an imbibition curve can be huge, because of this saturation difference in the transition zone. Furthermore, the amount of gas trapped in the residual gas zone, below the present day free water level, will still be influenced by depletion of reservoir pressure and hence, will provide energy to the producing reservoir, via either the brine phase or the gas phase. The residual gas bubbles will expand upon depletion and once a connected path flow is established, the gas will reconnect with the 'free' gas in the reservoir.

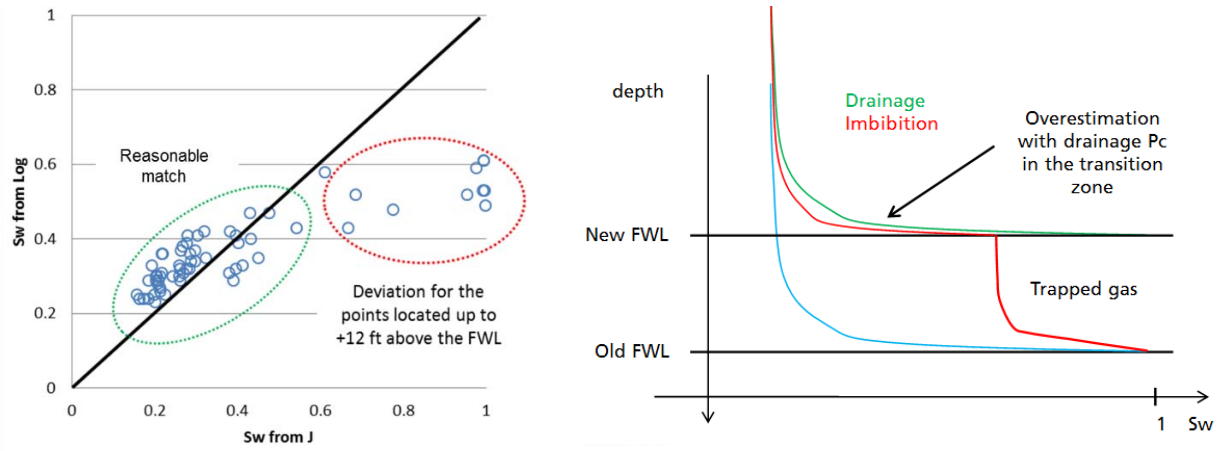

Figure 3: Example of paleo contact detected from a deviation of the saturation behavior in the transition zone

Sweep efficiency: because gas-water systems are always strongly water-wet and displacement is piston-like, the shape of Pc imbibition curve has little impact on the waterflood behavior, in terms of breakthrough time and pressure, except for the S_{gr} endpoint value. At (very) low injection rates, the core may spontaneously imbibe water, leading to negative pressure drops across the core.

In both cases, a preliminary estimate of the imbibition Pc curve can be obtained by rescaling the drainage curve between S_{wi} and S_{gr} as soon as the S_{gr} value is consistent (see next section). It is possible to infer the drainage curve by deriving the J-functions through

various standard techniques: HPMI (High Pressure Mercury Injection), centrifuge or porous plate.

In all the cases, the Pc curves to use for reservoir conditions purposes must account for both stress and interfacial tension using the Leverett formalism. Specific additional experiments are usually required like permeability-porosity as a function of stress and IFT data using either direct values from the pendant - ascending drop technique or estimates from PVT calculation, if the full gas and oil compositions are known. Among the 3 Pc techniques, porous plate is the only one to obtain direct relevant drainage Pc curves, if the experiments are conducted under full reservoir conditions. Usually the 3 approaches compare reasonably well for conventional gas-liquid reservoir systems: permeability > several mD (Sabatier, 1994) and the HPMI - centrifuge corrected curves can often be considered as a fair estimate whilst awaiting the porous plate results, which can take several months.

Residual Gas Saturation: S_{gr} is one of the most important parameters to acquire for an imbibition liquid-gas scenario, because it controls both the final saturation state and the dynamic behavior, since the displacement is piston-like (hence S_{gr} affects the breakthrough time). Representative S_{gr} values may be acquired from coreflood experiments conducted under stress, with some pore pressure to limit gas compressibility effects (see section on relative permeability endpoints). S_{gr} can be calculated by simple material balance (volumetric or gravimetric) and/or direct measurements using *in-situ* saturation monitoring (ISSM), which gives the added bonus of observing saturation as a function of sample length; although, uncertainties can be as high as several saturation units (s.u.), especially at reservoir conditions (Cense *et al.*, 2014). In general, S_{gr} values range between 20 and 40 s.u., where such inaccuracy can lead to errors typically in the range of 3% original GIP. It is therefore of primary importance to use several approaches for QC evaluations.

Firstly, include a compressibility test in the protocol after imbibition, in order to directly evaluate the remaining gas volume in the sample. Close the sample outlet and inject the imbibition test liquid until a predetermined pressure is achieved. Since pressure increase is linked directly to gas compression, induced by the liquid volume increase, it enables determination of the gas volume in place using the perfect or real gas law, dependent upon the fluid system.

$$P^{test}\left(V_{gas}^{ini} - V_{liq}^{inj}\right) = P^{ini}\,V_{gas}^{ini} \qquad V_{gas}^{ini} = \frac{P^{test}\,V_{liq}^{inj}}{(P^{test} - P^{ini})} \qquad S_{gr} = \frac{V_{gas}^{ini}}{PV}$$

With P^{ini} and P^{test} respectively, the initial pressure and stabilized pressure after injection, V_{gas}^{ini} the initial gas volume (prior to compressibility test), V_{liq}^{inj} the volume of liquid injected and PV the pore volume. This simple technique can give an additional and independent evaluation of S_{gr} very rapidly after the experiment.

Secondly, compare the results with published compilations of S_{gr}^{M} (maximum S_{gr} obtained with S_{wi} equal to 0) acquired from various samples (Suzanne, 2003; Pentland, 2010). As S_{gr} must be compared with SgrM, the Land equation (1971) can be used for the conversion, using default values of the Land constant according to the rock type (Irwin and Baticky, 1997).

Thirdly, conduct a large number of ambient conditions S_{gr}^{M} experiments in parallel to the few imbibition coreflood experiments planned. These experiments are simple, fast and relatively cheap to conduct. Clean samples are dried at 60°C and weighed. Immerse individual samples in a beaker of brine for roughly one hour for standard permeability (longer times may begin to introduce artefacts linked to gas dissolution, (Suzanne, 2003)). Alternatively, monitor immersed weight as a function of time, to the point of inflexion. After imbibition, take the samples from the beaker, remove superficial water and weigh. S_{gr}^{M} is calculated as the weight difference from dry state.

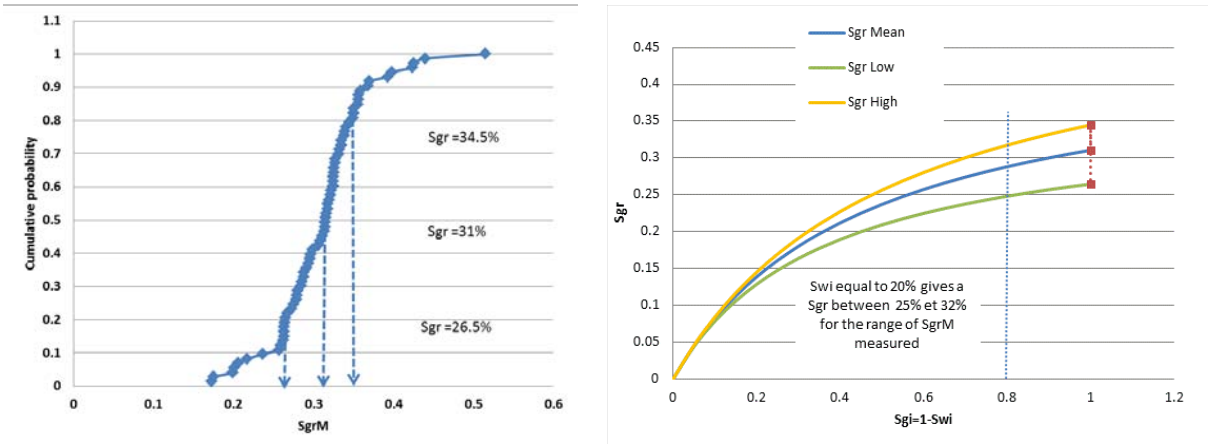

Figure 4: Probability curve of S_{gr}^{M} obtained from 73 measurements (left) and derived S_{gr} values using Land (1971)

An example of this approach is provided in Figure 4 (above), where an S_{gr}^{M} cumulative probability curve was obtained from 73 measurements on the same facies. It enabled definition of P50 and the associated variability. Using the Land equation (Land, 1971) and a representative S_{wi} value (20% considered in this example), it was possible to derive the range of expected S_{gr} values and to compare them with those obtained during the coreflood experiments. Another benefit of this approach is that the cumulative probability curve can be used to define the range of variation of the S_{gr} parameter, if the reservoir model is history matched through an automatic process.

The Brooks & Corey formalism (1966) is very attractive in the case of gas-liquid systems, since there is no ambiguity about the wettability. Drainage Pc data (mercury injection, centrifuge or porous plate) are first matched using the parametric law:

$$\left(\frac{P_d}{P_c}\right)^{\lambda} = \frac{S_w - S_r}{100 - S_r} = S_w^*$$

where P_d is the threshold pressure, λ rules the shape of the curve and represents the throat size distribution, S_r is the residual saturation. Once matched, the drainage gas-liquid relative permeability curves can be deduced in a straightforward manner using the following formulae:

$$K_{rw} = (S_w^*)^{\frac{2+3\lambda}{\lambda}} \quad and \quad K_{rnw} = (1-S_w^*)^2(1-S_w^{*\frac{2+\lambda}{\lambda}})$$

Although not reported explicitly in the literature, the Brooks and Corey approach (1966) can be easily applied to analyze imbibition data just by coupling the non-wetting phase trapping formula introduced by Land (1971) with a Carlson type hysteresis model (Carlson, 1981). For KrgI (imbibition), we use the above equation for drainage (D) in parallel with $K_{rg}I(S_g) = K_{rg}D(S_{gf})$, S_{gf} being the free gas saturation given from Land equation through the relation $S_{gf} = \frac{1}{2}\left[(S_g - S_{gr}) + \sqrt{(S_g - S_{gr})^2 - \frac{4}{C}(S_g - S_{gr})}\right]$

The Land formula must be calibrated to obtain the C constant representative of the facies under concern, where: $\frac{1}{S_{gr}} - \frac{1}{S_{gi}} = C$

Once calibrated (C, S_{wi} and λ), it is possible to assess the imbibition relative permeability curves and especially the endpoints. Figure 5 shows an example of qualitative QC using this approach on the endpoints of gas-brine relative permeability data. The blue and red curves provide the range of the expected $K_{rw}@S_{wi}$ and $K_{rg}@S_{gr}$ values, respectively. In this case, several outliers can be easily detected for further analysis of the raw data and interpretation.

Another practical approach is to compare relative permeability data from independent techniques. When Pc data are obtained from centrifuge, for example, it is recommended to spend some extra time to interpret the relative permeability curve of the displaced fluid in order to compare it with the one obtained from displacement technique (SS or USS). Where good agreement is observed, it adds confidence to the shape of the relative permeability curves, especially at late saturation, as depicted by the example provided in Figure 5 (right).

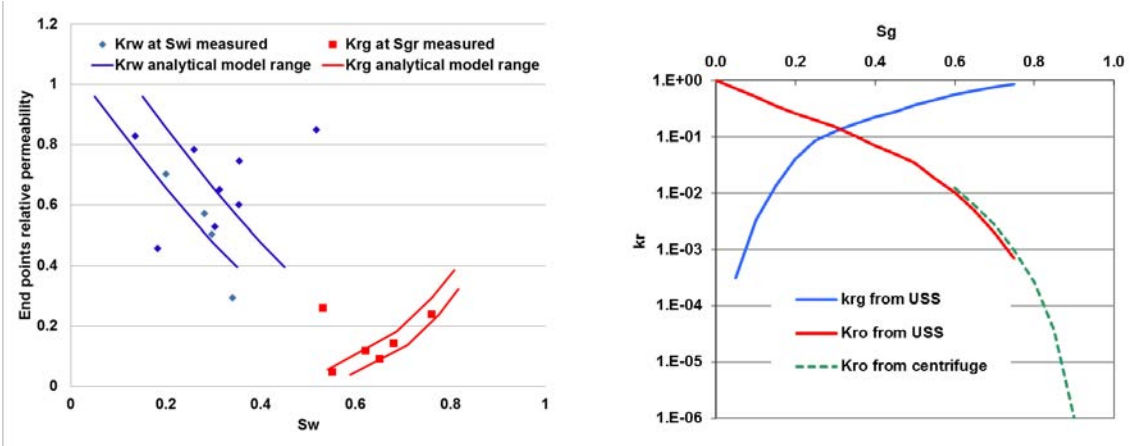

Figure 5: Quality control of endpoint relative permeability using Brooks and Corey type approach (1966) (left) – comparison between USS and centrifuge data for QC purpose (right)

Low Rate Waterflooding – Unsteady State

Bull *et al.*, 2011 presented data indicating that S_{gr} was a function of injection rate and recommended that residual gas measurements be performed at elevated or reservoir pressure to minimize gas compression and diffusion effects. However, many laboratories continue to perform analyses with little consideration of the implications of injection rate, compressibility and disequilibria (i.e. gas and water are not in full equilibrium due to pressure differentials required for flooding). Pore pressure for these tests in commercial labs, is often between 200-300 psi (15-20 bar) because of the pressure limitations of the graduated glass separators used to measure volumetric changes of the fluids. ISSM is always recommended as a secondary, verifying measurement method.

A number of unsteady state waterflood displacements to S_{gr} were reviewed. Pore pressures were 200 psi for all samples. Water injection rates varied from 0.5-4 ml/min, with little correlation to core properties. Figure 6 is a plot of permeability (normalized for area and length) against flow rates employed by a single lab during two projects from the same field, indicating the diversity and ill-considered rates employed. Figure 7 depicts a plot of S_{gr} versus water differential pressure (DP) after breakthrough for these samples. There is an obvious decline in residual gas saturation once DP exceeded 10 psi (5% of the applied pore pressure). This data confirms recommendations to limit differential pressure as a function of applied pore pressure (McPhee *et al.*, 2015), though the book states a more stringent limit of 2% pore pressure.

Low rate flooding experiments are performed to obtain S_{gr} values for cores initialized at representative S_{wi} (by porous plate or by centrifuge). When performing a waterflood on a gas filled core at S_{wi}, the gas volume produced equals the water volume injected until breakthrough. At breakthrough, gas saturation is observed to be residual throughout the core, and thus, no further gas production is expected after breakthrough.

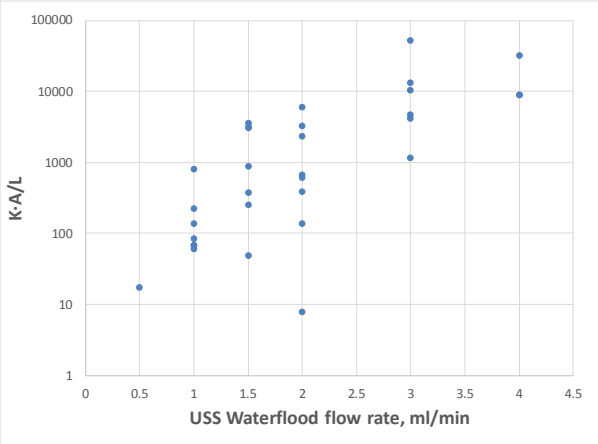

Figure 6: Permeability (normalized for Area & Length) versus Lab applied flow rates.

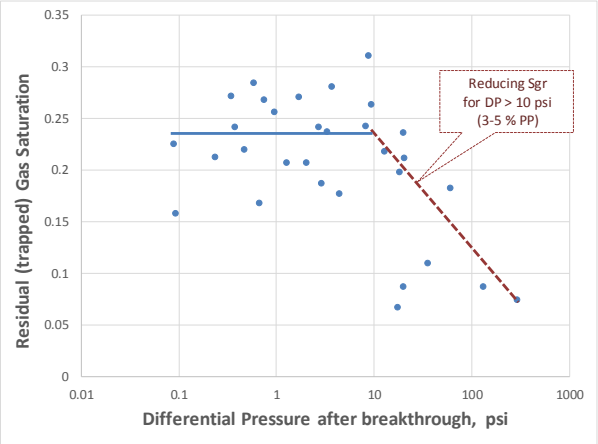

Figure 7: Sgr versus DP measured during post-breakthrough waterflooding

However, in some experiments, gas production continued after breakthrough. Plotting gas production as a function of brine pore volumes injected (PVI), an average (4 experiments) 2.9 ml additional gas was produced after approximately 30 PVI (ca. 400 ml) of brine after breakthrough (see Figure 8 (left)). Gas production was confirmed by ISSM. At breakthrough, the profiles were flat, i.e. the water saturation in the core is constant. After flooding multiple pore volumes, the water saturation has increased throughout the core, but more at the inlet than at the outlet.

Once brine is injected in the core, the pressure increases from 20 bar (back pressure of the whole system) to an injection pressure between 20.01 and 20.08 bar (differential pressure of 0.01-0.08 bar). Due to the higher inlet pressure, more nitrogen can be dissolved in the brine. The dissolved nitrogen will be evolved downstream of the core as pressure drops towards 20 bar again. It will either be trapped as residual gas, or surplus gas will be produced by viscous forces of the flowing brine.

In an attempt to quantifying this effect, an average pressure increase of 0.04 bar (4000 Pa) was assumed. The increased pressure leads to a concentration change of 4000 Pa / ($155 \cdot 10^6$ Pa / (mol/l) [Wilhelm et al. (1977)] = $2.58 \cdot 10^{-5}$ mmol/l. The amount of nitrogen lost during 400 ml of brine flushing through, at the inlet of the core is $1.03 \cdot 10^{-5}$ mmol, at room temperature and 20 bar pressure $1.3 \cdot 10^{-5}$ ml of nitrogen. This volume loss is orders of magnitude lower than the observed loss of 2.9 ml of nitrogen.

Another effect contributing to the gas stripping at the inlet happens when small amounts of gas are dissolved in the by-passing brine, which is under saturated: the size of the trapped gas bubbles is reduced, and as a consequence the local capillary pressure increases as the capillary pressure is proportional to the local curvature of the gas bubbles. This increases the local gas pressure and leads to gas dissolution, further decreasing the bubble size.

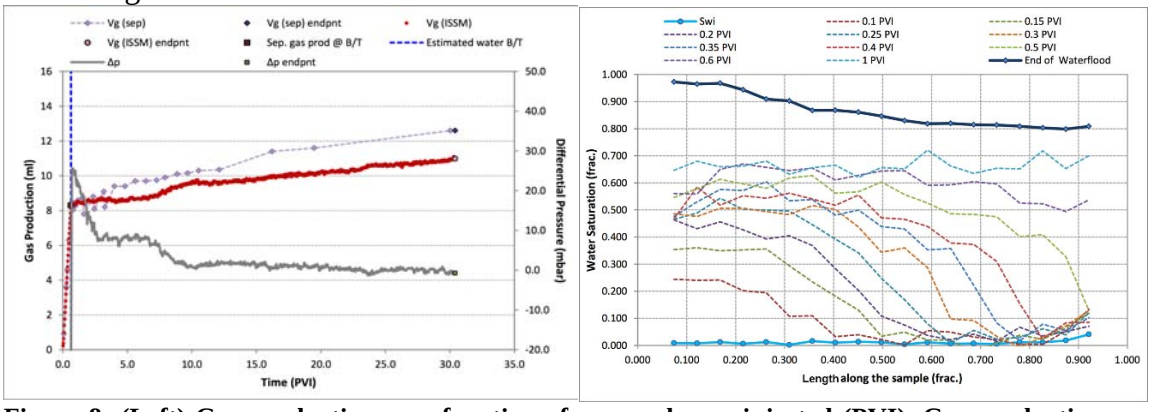

Figure 8: (Left) Gas production as a function of pore volumes injected (PVI). Gas production was measured using gamma ray (red line) & separator (dotted purple line). Pressure drop across the core in grey. (Right) Water saturation as a function of distance from inlet. Flooding from left to right.

In these experiments, the brine-nitrogen system was equilibrated for 24 hours by bubbling the nitrogen through the brine and the pore pressure was 100 bar. In another experiment, where the pore pressure was 5 bar and the equilibration time was 18 days, we did not observe any production of gas after breakthrough, which leads to the conclusion that 24 hours is not long enough to equilibrate nitrogen and brine from atmospheric pressure to 20 bar.

The tail end production of gas is thus considered to be an experimental artifact. The residual gas saturation representative for the reservoir is the residual gas saturation at breakthrough. It is our recommendation that USS waterfloods be performed at equivalent reservoir advancement rates (if the DP limits allow, else lower rates may be required), at limited differential pressure (max 5% of pore pressure) and for a limited injection volume, maximum 2 PVI.

Steady State Waterflooding

Steady state water displacing gas experiments are not generally recommended as a method to acquire imbibition water-gas relative permeability data; unless one is aware of the limited saturation range expected from these analyses and of the potential saturation inaccuracies because of disequilibria effects, or unless one has access to appropriate equipment and expertise, together with sufficient time and budget.

Figure 9 provides two plots from an imbibition water-gas steady state relative permeability test. These plots depict the correlation between anomalous, non-uniform saturation profiles (left) and differential pressures measured during each fractional flow rate of the test (right), plotted as a function of pore volumes water injected (PVI). Water saturation begins from S_{wi} = 0.163 and increases to S_w = 0.505 during the first fractional water flow (f_w=0.003). This is an increase of 34.5 saturation units (s.u.) at a very low fractional flow rate and represents one of the lowest viable fractional rates for most commercial laboratories (equipment and time limitations). Saturation is relatively uniform after this first fractional rate, and after the subsequent two fractions. However, after f_w=0.201, where DP increases above 10 psi, and above 5% pore pressure, a significant decreasing saturation gradient is observed from injection to production face (0 to 1 fractional length). The gradient increases during the next two fractional flow rates because of increased DP and greater water throughput. This results in inaccurate saturation data for the last three fractions and a poorly defined relative permeability saturation range, which defeats the purpose of the steady state method, since a major objective is to define a wider relative permeability saturation range than obtained by the unsteady state method.

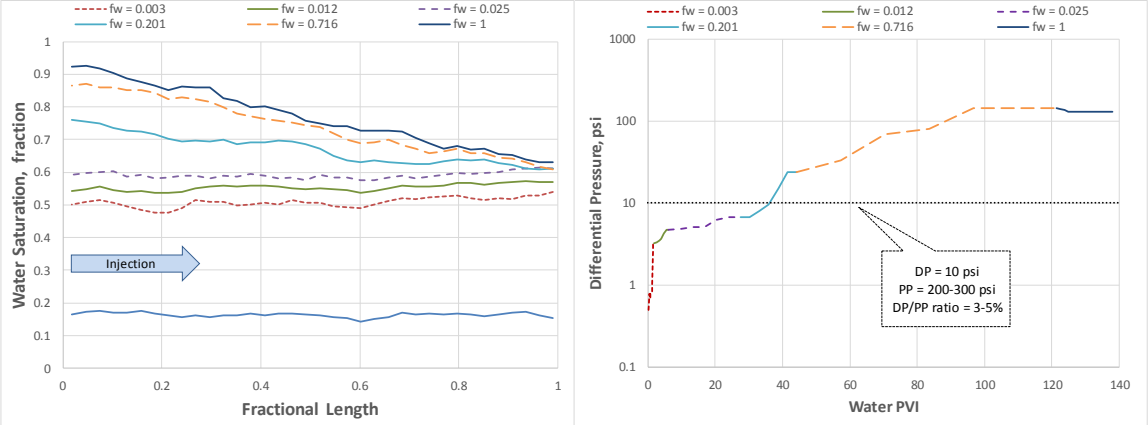

Figure 9: DP versus water PVI during an imbibition steady state waterflood (left). Resultant ISSM profiles during this experiment, depicting disequilibria effects at the sample injection face.

The analyses are controlled strongly by imbibition capillary pressures, resulting in the observed large encroachment of water saturation at very low fractional water flow rates. The large saturation increase is unavoidable. Fractional flow rates require to be some orders of magnitude lower, which would require either, ultra-low water flow rates (hence extremely long experimental times), or higher total injection rates (requiring very high gas injection rates, which risk extending into turbulent flow regimes).

Simulations of these steady state experiments were performed in an attempt to determine potential experimental parameters that might provide reasonable results within the limitations described earlier for standard commercial laboratory equipment, at ambient temperature and pore pressures of approximately 300 psi (20 bar).

Corey functions of N_g=2, N_w=5, endpoint k_{rw}=0.1 and S_{gr}=0.25 were used together with imbibition Pc data, modified from MICP curves, for a sample permeability range from 1-100 mD. Simulation using an initial fractional flow rate of f_w=0.0001, approximately a magnitude lower than the SS experimental data above, resulted in the saturation profiles given in Figure 10, for the 100 mD case. In this case, there was still a significant saturation change (over 35 s.u.) during that first, low f_w step. The first f_w step was estimated to require approximately 10 days to stabilize. A further, magnitude-lower f_w was estimated to require over 30 days to stabilize during the first f_w. Such stabilization times are uneconomical for both laboratory and client company, hence unfeasible. It was also noted that saturation after subsequent f_w steps was observed, at best, to cover a 25 s.u. range.

In addition to these undesirable saturation changes, the high throughput volumes required during a steady state test lead to a greater potential for disequilibria effects. Initially, at low f_w, differential pressure is low because gas viscosity is the main flowing phase; however, as f_w increases, DP will increase and may exceed the DP limits described above. This may be regulated by decreasing the total injection rate at each increasing f_w.

It is therefore recommended that, if employing gas-liquid SS testing (given the inherent issues), DP should be minimized in this manner.

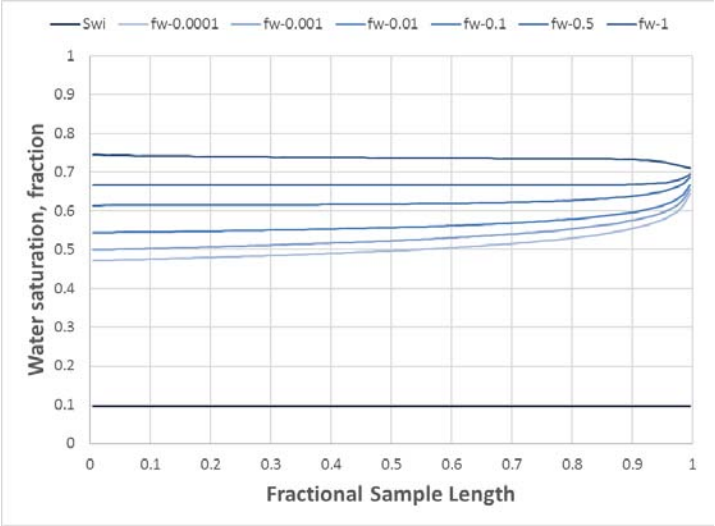

Figure 10: Example of simulated saturation profiles for SS water-gas relative permeability

CONCLUSIONS

In this paper we have discussed common pitfalls that may arise when conducting gas water SCAL experiments. The difference between drainage and imbibition processes can lead to an evaluation of too low gas saturation in place. This may be determined if there is no match between log saturations and those inferred from drainage models or if there is a deviation from J-function saturations. The porous plate technique is recommended as it can measure the Pc curves at full reservoir conditions. However, mercury-air or centrifuge measurements are much quicker to perform, and give reasonably reliable data.

It is recommended to use reservoir equivalent advancement rates (low rate) for corefloods to S_{gr}. Fluid equilibration time, between gas and brine, is important prior to conducting flooding experiments. It is recommended to limit differential pressures during low rate corefloods, and limit injection to two pore volumes. It is recommended to compare and quality control S_{gr} from (low rate) coreflood experiments, using ISSM, other volumetric methods, and published and measured values for S_{gr}^{M}. Relative permeability endpoints should be checked for outliers using an analytical approach that helps in determining confidence intervals.

Water-gas imbibition steady state experiments are not recommended when using the limited equipment of most commercial laboratories, unless one is aware of the limitations and cost implications of performing these tests, or one has equipment and expertise appropriate to acquiring these data.

REFERENCES

1. Brooks, R. H. and Corey, A. T.: "Properties of Porous Media Affecting Fluid Flow", J. Irrig. Drain. Div., (1966), 6, 61.
2. Land, C.: “Comparison of Calculated with Experimental Imbibition Relative Permeability”, Society of Petroleum Engineers Journal, vol. 11, no. 4, pp. 419-425, 1971.
3. Pentland, C.H.: “Measurements of Non-Wetting Phase Trapping in Porous Media”, PhD, Imperial College, November 2010.
4. Sabatier, L.: “Comparative study of drainage capillary pressure measurements using different techniques and for different fluid systems”, SCA-9424.
5. Suzanne, K.: “Evaluation of the trapped gas saturation in water-wet sandstones – Influence of the rock properties and the initial saturation state”, PhD, Ecole des Mines de Paris, February 2003.
6. Honarpour, M. and Mahmood, S.M.: “Relative permeability measurements: an overview”, Journal of Petroleum Technology (1988), SPE 18565.
7. Jerauld, G.R.: “Prudhoe Bay Gas/Oil Relative Permeability”, SPE Reservoir Engineering, 1997
8. Cense, A.W., van der Linde, H.A., Brussee, N., Beljaars, J., Schwing, A.: “How reliable is in situ saturation monitoring (ISSM) using X-ray?”, SCA-2014-09.
9. Wilhelm, E., Battino, R., Wilcock, R.J.: “Low-pressure solubility of gases in liquid water.” J Chem. Rev., **77**, 219–262, 1977.
10. Goodman, J.B., Krase, N.W.: “Solubility of Nitrogen in Water at High Pressures and Temperatures” Industrial and Engineering Chemistry, 1931.
11. Bull, Ø., Bratteli, F., Ringen, J.K., Melhuus, K., Bye, A.L., Iversen, J.E.: “The Quest for True Residual Oil Saturation – An Experimental Approach”, SCA201103
12. McPhee, C., Reed, J., Zubizarreta, I. “Core Analysis: A Best Practice Guide”, chapter 10 about relative permeability, Developments in Petroleum Science, Elsevier, 2015, Volume 64, Pages 519-653.
13. Irwin D.D., Baticky J.P. “The successive displacement process: oil recovery during blowdown”, SPE 36719, November 1997, SPERE Journal.
14. Carlson F.M.: “Simulation of relative permeability hysteresis to the non-wetting phase”, SPE 10157, ATCE, San Antonio, Texas, 4-7 October 1981.